

Stereospecific Polymerization of Chiral Oxazolidinone-Functionalized Alkenes

Garret M. Miyake, Daniel A. DiRocco, Qin Liu, Kevin M. Oberg, Ercan Bayram, Richard G. Finke, Tomislav Rovis, and Eugene Y.-X. Chen*

Department of Chemistry, Colorado State University, Fort Collins, Colorado 80523-1872

Received June 14, 2010; Revised Manuscript Received August 9, 2010

ABSTRACT: Acryloyl and vinyl monomers functionalized with a chiral oxazolidinone auxiliary have been successfully polymerized in a stereospecific fashion to highly isotactic, optically active polymers, through either the previously established isospecific coordination polymerization (for acryloyl monomers) or a novel isospecific cationic polymerization (for vinyl monomers). Specifically, conjugated chiral acryloyloxazolidinones, *N*-acryloyl-(*R* or *S*)-4-phenyl-2-oxazolidinone [(*R* or *S*)-AOZ], are readily polymerized by chiral *ansa*-zirconocenium coordination catalysts, (*R,R*-, *S,S*-, or *R,R/S,S*)-[C₂H₄(η⁵-Ind)₂]Zr⁺(THF)[OC(OⁱPr)=CMe₂][MeB(C₆F₅)₃][−] (**1**), in an isospecific manner through a catalyst-site-controlled mechanism, producing the corresponding optically active chiral polymers, (*R* or *S*)-PAOZ. Owing to the nature of stereocontrol dictated by the chiral catalyst site, even the coordination polymerization of the parent AOZ, without the chiral side group, also affords PAOZ with nearly quantitative isotacticity. A series of experiments have shown that the chiral polymers (*R* or *S*)-PAOZ exhibit no chiral amplifications, despite having stereoregularly placed stereogenic centers in the main chain, and the optical activity of the polymers arises solely from their chiral auxiliary, a consequence of adopting a random-coil secondary structure and thus having a cryptochiral chain. In sharp contrast, the chiral isotactic polymers derived from nonconjugated chiral vinyl oxazolidinones, *N*-vinyl-(*R*)-4-phenyl-2-oxazolidinone [(*R*)-VOZ] and its *p*-hexyloxyphenyl derivative (*R*)-HVOZ (designed to solve the solubility issue of the resulting polymer), exhibit substantial chiral amplifications by virtue of adopting a solution-stable, one-handed helical conformation. The synthesis of such helical vinyl polymers has been accomplished by the development of a novel isospecific cationic polymerization using Lewis and Brønsted acids, such as [Ph₃C][B(C₆F₅)₄], BF₃·Et₂O, and [H(Et₂O)₂][B(C₆F₅)₄], through a chiral auxiliary-controlled mechanism. Noteworthy is the combination of the near-quantitative isotactic placement of the stereogenic centers of the polymer main chain with the chiral side groups located near those stereocenters that renders one-handed helicity of (*R*)-PVOZ and (*R*)-PHVOZ. Significantly, this novel cationic polymerization process, operating at ambient temperature, effectively assembles two elements of polymer local chirality—side-chain chirality and main-chain chirality—into global chirality in the form of excess one-handed helicity. Furthermore, the resulting chiral helical vinyl polymers exhibit considerably higher thermal decomposition temperatures and polymer crystallinity, in comparison to the random-coil chiral acryloyl polymers, having a similarly high degree of main-chain stereoregularity.

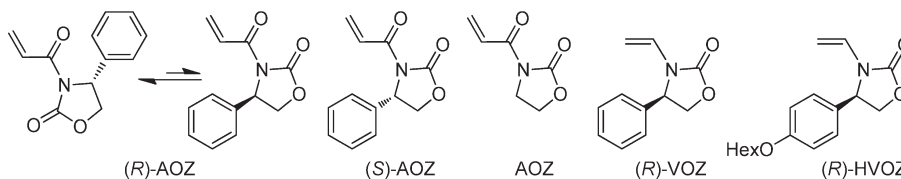
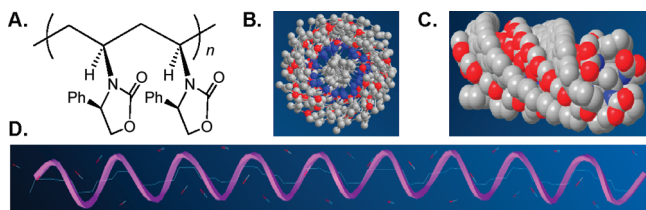
Introduction

Optically active synthetic polymers are of considerable current interest.¹ Such polymers are not only fundamentally intriguing (due to their rich and complex architectures derived from macromolecular chirality that diverges from that of small molecule chirality) but are also technologically important (due to their unique chiral arrays that give rise to a number of potential, and in some cases commercially implemented, applications such as chiral separation).¹ We are particularly interested in the utilization of chiral N,O-functionalized polar vinyl polymers² as potential chiral polymeric ligands/stabilizers for transition metal nanocluster catalysts³ en route to asymmetric catalysis.⁴ This interest stems from the observation that N,O-functionalized polar vinyl polymers, such as poly(vinylpyrrolidone) (PVP), are among the most common, effective stabilizers for transition-metal nanoclusters⁵ and the reasoning that chiral polymers have the suitable length scale and binding rigidity as well as “high chirality”⁶ that can match the extended surface of the nanoclusters. However, optically active PVP is not accessible; even if enantiomerically pure or

enriched stereoregular PVP is synthesized, such a vinyl polymer with configurational main-chain chirality without chiral side groups *cannot* be optically active since the entire polymer chain (by the infinite chain model) contains a mirror plane (for isotactic polymers) or a glide mirror plane and translational mirror planes perpendicular to the chain axis (for syndiotactic polymers).^{1j,i} On the other hand, a polymer assuming a one-handed helical conformation is inherently chiral.¹ Many polymers are known to form a helical structure in the solid state; however, they typically adopt optically inactive, on-average random-coil conformations in solution due to fast solution dynamics of the polymer chain with low helix-inversion barriers. Our MM2 modeling indicated that isotactic PVP would adopt a random-coil conformation, suggesting that enantiomeric chiral PVP with appreciable molecular weight (MW), if synthesized, would be optically inactive. In short, there exists a need for the synthesis of optically active, chiral PVP variants.

A solution to this fundamental problem is to install a chiral auxiliary into conjugated or nonconjugated vinyl monomers which, upon polymerization, will lead to optically active polymers. If such polymerization proceeds in a stereospecific manner,

*Corresponding author. E-mail: eugene.chen@colostate.edu.

Chart 1. Structures of Chiral 2-Oxazolidinone-Functionalized Conjugated Acrylamide and Nonconjugated Vinyl Monomers Employed in This Study**Chart 2. Primary Structure of (R)-PVOZ (A) as Well as MM2-Calculated 4_1 Helical Structure of [(R)-VOZ] $_{30}$, Shown from Top (B), Side (C), and Ribbon (D) Views^a**

^aCarbon, nitrogen, and oxygen are shown in gray, blue, and red, respectively; hydrogen atoms are omitted for clarity.

then the resulting stereoregular polymers could attain additionally helical chirality due to control of the polymer secondary structure. Pino and Lorenzi first demonstrated that isotactic vinyl polymers bearing chiral side groups, such as poly(*S*)-3-methyl-1-pentene, can exist in solution with excess one-handed helicity and that the optical rotation of such polymers increased with increasing isotacticity.⁷ With this concept and the goal of this work in mind, three reasons led us to enantiomeric (*R* or *S*)-4-phenyl-2-oxazolidinone-functionalized conjugated and nonconjugated vinyl monomers *N*-acryloyl-(*R* or *S*)-4-phenyl-2-oxazolidinone [(*R* or *S*)-AOZ] and *N*-vinyl-(*R*)-4-phenyl-2-oxazolidinone [(*R*)-VOZ] (Chart 1). First, the chiral oxazolidinone group has been used as a chiral auxiliary in organic synthesis for over 30 years.⁸ Second, the resulting N,O-functionalized chiral polymers, (*R* or *S*)-PAOZ and (*R*)-PVOZ, structurally resemble that of PVP, in addition to being optically active. Third, introduction of the phenyl group at the 4-position of the oxazolidinone ring could sterically induce a solution-stable helical conformation of the isotactic polymer, thereby effectively assembling two elements of local chirality—side-chain chirality (stereocenters at 4-positions of the side chain) and main-chain chirality (stereocenters generated at 2-vinyl carbon positions during stereoselective polymerization)—into global chirality (formation of excess one-handed helicity). Indeed, MM2 modeling of the isotactic [(*R*)-VOZ] $_{30}$ predicts a chiral 4_1 helical structure (Chart 2).

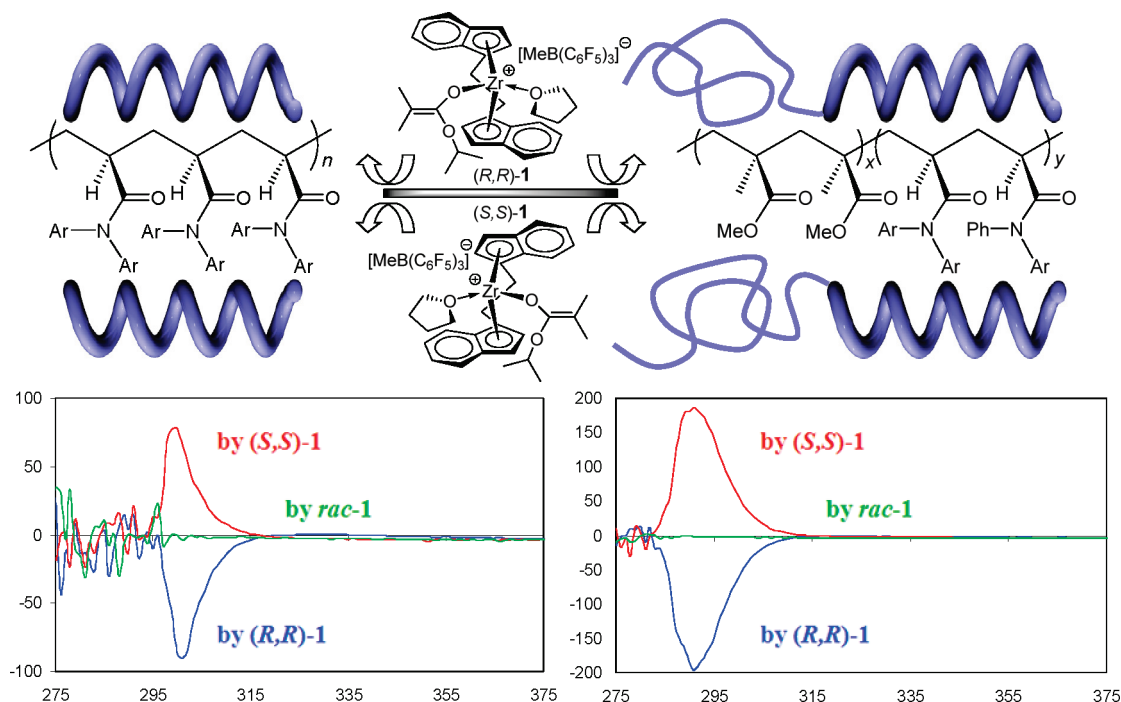
Free-radical polymerization has been previously employed to polymerize conjugated vinyl monomers bearing chiral auxiliary groups stereoselectively.⁹ However, due to unfavorable dipole interactions between the oxazolidinone and acryloyl carbonyls, conjugated AOZ with a chiral auxiliary at the 4-position favors a rotamer which shields the auxiliary away from the reactive center (cf. left rotamer of (*R*)-AOZ, Chart 1), providing little stereochemical control in additions to the C=C bond.¹⁰ Using a suitable Lewis acid (LA), such as Sc(OTf) $_3$, should lock the auxiliary in the preferred conformation for control of stereochemistry (cf. right rotamer of (*R*)-AOZ, Chart 1) through bidentate chelation of the LA to both carbonyls of the monomer; however, such complexation renders the radical and monomer too electron-deficient to react efficiently for homopolymerizations. Nevertheless, (4*S*)-AOZ can be radically copolymerized with electron-rich isobutylene in the presence of a LA, yielding isotactic alternating copolymer with a *m/r* dyad ratio of >95:5.¹⁰ In the case of chiral oxazolidinone acrylamides, stereocontrolled (through chiral auxiliary control¹¹) free-radical polymerization

has been achieved without LA additives, producing isotactic polymers with a *m/r* dyad ratio reaching 92:8.¹² Interestingly, the nonconjugated, unsubstituted VOZ undergoes rapid decomposition (devinylation) to 2-oxazolidinone and acetaldehyde in acidic aqueous solution with pH < 4.0 so that the radical polymerization in the presence of poly(methacrylic acid) was successful only at pH \geq 4.0.¹³ This monomer, upon free-radical polymerization by AIBN, was reported to form water-soluble polymers with MW ranging from 450 to 100 000 (by microisopiestic measurements)¹⁴ or a water-insoluble polymer which decomposes at \sim 300 °C without melting. An attempt to polymerize this monomer by a Ziegler–Natta coordination catalyst (TiCl $_3$ /HONH $_3^+$ Cl $^-$) led to no polymer formation, but instead the acid-catalyzed devinylation product.¹⁵ Acid-catalyzed devinylation of *N*-vinyl heterocyclic monomers has also been noted elsewhere.¹⁶ VOZ monomers having alkyl or phenyl substituents at 5-positions can be polymerized by AIBN in dioxane or in bulk.¹⁷ The polymers derived from radical polymerization of VOZ monomers are essentially atactic.¹⁸

As can be seen from the above overview, AOZ and VOZ monomers have previously been successfully polymerized only by radical polymerization methods, while the polymerization of (4*R* or 4*S*)-VOZ monomers of our current interest has not been reported. Furthermore, chiral auxiliary-controlled radical polymerization has led to formation of an isotactic copolymer of (4*S*)-AOZ with isobutylene, but the isotactic homopolymer of (4*R* or 4*S*)-AOZ of interest herein was previously unknown. Lastly, no stereoregular polymers derived from VOZ monomers have been reported.

We hypothesized that the synthetic challenges identified above could be met by employing isospecific, enantiomeric (*R,R* or *S,S*)-ansa-metalocenium coordination catalysts that were recently developed for the asymmetric coordination polymerization of functionalized vinyl monomers such as prochiral acrylamides leading to optically active, helical vinyl polymers.¹⁹ Our reasoning is threefold: First, we have already shown that catalyst **1** polymerizes prochiral conjugated acrylamides with bulky substituents, such as *N,N*-diarylacrylamides, to highly isotactic, chiral polymers adopting a solution-stable, one-handed-helical conformation, where the handedness of the helix is dictated by the chirality of the catalyst (Chart 3).¹⁹ In contrast, if the monomer is not sufficiently sterically bulky [i.e., methyl methacrylate (MMA)], the resulting polymer does not form a solution-stable helix, but instead a random coil conformation. Such low-MW enantiomeric oligomers can exhibit some optical activity arising from the absence of mirror planes due to nonequivalent chain-end groups, but as the MW increases, the effects of the chain-end groups on the chiroptical properties of the polymers diminish so that the optical activity decreases to null as the polymer becomes cryptochiral.^{20,21} Second, we reasoned that the zirconocene ester enolate cation **1** can serve as both initiator (the enolate ligand as nucleophile) and LA catalyst as chelator for the two carbonyls in the AOZ monomer,²² thus rendering both high activity and high stereochemical control in AOZ polymerization (vide supra). Studies in the polymerization of chiral AOZ monomers by the enantiomeric catalysts **1** will determine if they can produce isolable, right- and left-handed, solution-stable helical polymers bearing the same chiral auxiliary, trapped in a kinetically

Chart 3. Asymmetric Polymerization by Enantiomeric Catalysts 1 for the Synthesis of Right- and Left-Handed Helical Poly[*N*-phenyl-*N*-(4-tolyl)acrylamide)s and Their Block Copolymers with MMA^a



^a Shown on the bottom are the CD spectra of homopolymers and block copolymers by (S,S)-1 (red), *rac*-1 (green), and (R,R)-1 (blue).^{19,20}

stable state—a case of catalyst site control. Comparative studies using the racemic catalyst and other catalysts with different stereochemical control will also reveal whether the chiral auxiliary will dictate the handedness of the helix, either through an initial formation of a preferred single-handed helix or through a thermodynamic mutarotation to the preferred helical conformation—the case of chiral auxiliary control. Third, we reasoned that being a class of electron-rich monomers, chiral VOZ could be cationically polymerized by metallocene or other related cations and isospecificity rendered by the chiral auxiliary, if devinylation is overcome by appropriate strategies such as spontaneous polymer precipitation. As indicated in Chart 2, highly isotactic (*R*)-PVOZ will most likely adopt a solution-stable helical structure, thereby accomplishing our goal of synthesizing those needed optically active polymers. Herein we report our findings in testing each of these three hypotheses.

Experimental Section

Materials, Reagents, and Methods. All syntheses and manipulations of air- and moisture-sensitive materials were carried out in flame-dried Schlenk-type glassware on a dual-manifold Schlenk line, a high-vacuum line, or in an argon or nitrogen-filled glovebox. HPLC-grade, nonstabilized organic solvents were sparged extensively with nitrogen during filling of the solvent reservoir and then dried by passage through activated alumina (for THF, Et₂O, and CH₂Cl₂) followed by passage through Q-5-supported copper catalyst (for toluene and hexanes) stainless steel columns. HPLC-grade DMF was degassed and dried over CaH₂ overnight, followed by vacuum transfer. Toluene-*d*₈ and benzene-*d*₆ were degassed, dried over sodium/potassium alloy, and filtered before use, whereas CDCl₃, CD₂Cl₂, and DMSO-*d*₆ were degassed and dried over activated Davison 4 Å molecular sieves. NMR spectra were recorded on a Varian Inova 300, 400, or 500 MHz (for polymer tacticity analysis) spectrometer. Chemical shifts for ¹H and ¹³C spectra were referenced to internal solvent resonances and are reported as parts per million relative to tetramethylsilane, whereas ¹⁹F NMR spectra were referenced to external CFCl₃.

Acetaldehyde diethyl acetal, aniline, ⁿBuLi (1.6 M in hexanes), butylated hydroxytoluene (BHT-H, 2,6-di-*tert*-butyl-4-methylphenol), camphorsulfonic acid, 1,2-dibromobenzene, 1,2-dibromoethane, diisopropylamine, indene, lithium dimethylamide, (2*S*,4*S*)-pentanediol (99% *ee*, [α]_D²⁰ +39.8, *c* = 10, CHCl₃), (2*R*,4*R*)-pentanediol (97% *ee*, [α]_D²¹ -40.4, *c* = 10, CHCl₃), sodium azide, tetrachlorozirconium, 1,1,3,3-tetramethylguanidine, triethylamine, and triflic acid as well as (CF₃SO₂)₂O, PhBCl₂, MeMgI (3.0 M in diethyl ether), BF₃·Et₂O, ^tBu₃Al (neat), AIBN, and CF₃COOH were purchased from Aldrich. MMAO (2.2 wt % Al in heptane) was purchased from Akzo Nobel. Acryloyl chloride and 2,6-dimethylpyridine were purchased from Alfa Aesar. Trimethylaluminum (neat) was purchased from Strem Chemical Co., whereas (*S*)- and (*R*)-4-phenyl-2-oxazolidinone, isopropyl isobutyrate, and *N*-methylaniline were purchased from TCI America. Indene, 1,2-dibromoethane, *N,N*-dimethylaniline, and acryloyl chloride were degassed using three freeze–pump–thaw cycles. Diisopropylamine, triethylamine, (CF₃SO₂)₂O, and PhBCl₂ were vacuum-distilled. 2,6-Dimethylpyridine, isopropyl isobutyrate, and aniline were degassed and dried over CaH₂ overnight, followed by vacuum distillation. BHT-H was recrystallized from hexanes prior to use. 1,4-Dioxane (Fisher Scientific) was degassed, dried over sodium/potassium alloy, and vacuum-distilled. All other commercial reagents were used as received.

Borate salts [Ph₃C][B(C₆F₅)₄] and [HN(Me)₂Ph][B(C₆F₅)₄] as well as borane B(C₆F₅)₃ were obtained as a research gift from Boulder Scientific Co.; the borane was further purified by recrystallization from hexanes at -35 °C. The (C₆F₅)₃B·THF adduct was prepared by addition of THF to a toluene solution of the borane followed by removal of the volatiles and drying in vacuo. Literature procedures were employed for the preparation of the following compounds and metallocene complexes: (*S*)-AOZ,²³ (*R*)-AOZ,²³ AOZ,²⁴ (*R*)-VOZ,²⁵ [H(Et₂O)₂]⁺[B(C₆F₅)₄]⁻,²⁶ LiOC(OⁱPr)=CMe₂,²⁷ (EBI)H₂ [EBI = C₂H₄(η⁵-Ind)₂],²⁸ *rac*-(EBI)Zr(NMe₂)₂,²⁹ *rac*-(EBI)ZrMe₂,²⁹ *rac*-(EBI)ZrMe(OTf),³⁰ *rac*-(EBI)ZrMe[OC(OⁱPr)=CMe₂],³⁰ *rac*-(EBI)Zr⁺(THF)[OC(OⁱPr)=CMe₂][MeB(C₆F₅)₃]⁻ (*rac*-1),³⁰ (*S,S*)-(EBI)ZrCl₂,³¹ (*R,R*)-(EBI)ZrCl₂,³¹ (*S,S*)-(EBI)ZrMe[OC(OⁱPr)=CMe₂],^{19,20} (*R,R*)-(EBI)ZrMe[OC(OⁱPr)=CMe₂],^{19,20} (*S,S*)-(1),^{19,20} and (*R,R*)-(1).^{19,20}

(*R*)-Methyl 2-((*tert*-Butoxycarbonyl)amino)-2-(4-(hexyloxy)phenyl)acetate. To a flame-dried flask with a magnetic stir bar was added (*R*)-methyl 2-((*tert*-butoxycarbonyl)amino)-2-(4-hydroxyphenyl)acetate (19.4 g, 68.8 mmol, 1.0 equiv), anhydrous K_2CO_3 (23.8 g, 172 mmol, 2.5 equiv), and anhydrous DMF (250 mL). The mixture solution was cooled to 0 °C, after which 1-iodohexane (25.4 mL, 172 mmol, 2.5 equiv) was added and the reaction was allowed to stir overnight at room temperature. Diethyl ether (1000 mL) was added, and the mixture washed with water (2 × 500 mL), saturated $KHSO_4$ (500 mL), and brine (500 mL). The solution was dried with $MgSO_4$ and concentrated to give a yellow oil which was purified by silica gel chromatography (9:1 hexanes:EtOAc) to yield the desired product as a clear oil (14.1 g, 56%). $R_f = 0.18$ (9:1 hexanes:EtOAc). $[\alpha]_D^{21} = -45.5$ ($c = 0.013$ g/mL, MeOH). 1H NMR (400 MHz, $CDCl_3$): δ 7.22 (d, $J = 8.5$ Hz, 2H), 6.82 (m, 2H), 5.44 (bd, $J = 6.4$ Hz, 1H), 5.21 (bd, $J = 7.2$ Hz, 2H), 3.90 (t, $J = 6.6$ Hz, 2H), 3.67 (s, 3H), 1.73 (m, 2H), 1.39 (s, 9H), 1.29 (m, 5H), 0.87 (m, 3H). ^{13}C NMR (100 MHz, $CDCl_3$): δ 172.1, 159.4, 155.0, 128.9, 128.5, 115.0, 80.2, 68.2, 57.2, 52.8, 31.7, 29.4, 28.5, 25.9, 22.8, 14.2. IR (NaCl, neat): 3440, 3380, 2955, 2933, 2872, 1747, 1717, 1612, 1511, 1247, 1169 cm^{-1} . HRMS (ESI+) calcd for $C_{20}H_{31}NNaO_5$: 365.2202; found: 365.2217.

(*R*)-4-(4-(Hexyloxy)phenyl)oxazolidin-2-one. To a solution of $LiAlH_4$ (1.61 g, 42.5 mmol, 1.1 equiv) in THF (200 mL) was added dropwise a solution of (*R*)-methyl 2-((*tert*-butoxycarbonyl)amino)-2-(4-(hexyloxy)phenyl)acetate (14.1 g, 38.7 mmol, 1.0 equiv) in THF (150 mL). The reaction was stirred at room temperature until the starting material was consumed by TLC analysis, after which 10% KOH was added and the reaction mixture filtered and concentrated to yield an off-white solid. The solid was dissolved in THF (400 mL) and cooled to 0 °C, after which thionyl chloride (22.4 mL, 309 mmol, 8.0 equiv) was added dropwise, and the solution was stirred for an additional 3 h at 0 °C, then warmed to room temperature, and stirred overnight. The reaction was concentrated to give a viscous oil that was crystallized with hexanes and filtered, yielding the desired product as a white amorphous solid (7.01 g, 68%). $R_f = 0.22$ (1:1 hexanes:EtOAc). $[\alpha]_D^{21} = -12.5$ ($c = 0.8$ g/dL, MeOH). 1H NMR (400 MHz, $CDCl_3$): δ 7.20 (m, 2H), 6.85 (m, 2H), 5.87 (bs, 1H), 4.86 (m, 1H), 4.64 (m, 1H), 4.12 (m, 1H), 3.91 (m, 2H), 1.74 (m, 2H), 1.42 (m, 2H), 1.29 (m, 4H), 0.87 (m, 3H). ^{13}C NMR (100 MHz, $CDCl_3$): δ 159.8, 159.7, 131.3, 127.5, 115.3, 72.9, 68.3, 56.2, 31.7, 29.3, 25.9, 22.8, 14.2. IR (NaCl, neat): 3284, 2932, 2860, 1756, 1613, 1514, 1246, 1032 cm^{-1} . HRMS (ESI+) calcd for $C_{15}H_{22}NO_3$: 263.1521; found: 263.1526.

(*R*)-4-(4-(Hexyloxy)phenyl)-3-vinylloxazolidin-2-one (HVOZ). To a flame-dried flask was added palladium(II) trifluoroacetate (63 mg, 0.19 mmol, 0.05 equiv), 1,10-phenanthroline (34 mg, 0.19 mmol, 0.05 equiv), and *n*-butyl vinyl ether (4.9 mL, 37.9 mmol, 10.0 equiv). This mixture was stirred for 5 min, followed by the addition of (*R*)-4-(4-(hexyloxy)phenyl)oxazolidin-2-one (1.0 g, 3.79 mmol, 1.0 equiv). The reaction was heated to 75 °C for 12 h, filtered through Celite, and concentrated. Purification of the crude product by silica gel chromatography gave a viscous oil which was crystallized with pentanes and filtered to yield the desired product as a white solid (1.07 g, 98%). $R_f = 0.15$ (9:1 hexanes:EtOAc). $[\alpha]_D^{21} = -44.8$ ($c = 1.70$ g/dL, CH_2Cl_2); mp (°C): 52–53. 1H NMR (400 MHz, $CDCl_3$): δ 7.14 (d, $J = 8.5$ Hz, 2H), 6.87 (d, $J = 8.4$ Hz, 2H), 6.77 (dd, $J = 16.0, 9.3$ Hz, 1H), 4.95 (dd, $J = 9.0, 5.4$ Hz, 1H), 4.66 (m, 1H), 4.28 (d, $J = 9.3$ Hz, 1H), 4.08 (m, 2H), 3.91 (t, $J = 6.5$ Hz, 2H), 1.74 (m, 2H), 1.42 (m, 2H), 1.30 (m, 4H), 0.87 (m, 3H). ^{13}C NMR (100 MHz, $CDCl_3$): δ 159.7, 155.9, 129.8, 129.0, 127.3, 115.4, 96.0, 71.0, 68.3, 58.0, 31.7, 29.4, 25.9, 22.8, 14.2. IR (NaCl, neat): 2932, 2871, 1765, 1639, 1613, 1514, 1394, 1246 cm^{-1} . HRMS (ESI+) calcd for $C_{17}H_{24}NO_3$: 289.1678; found 289.1679.

General Polymerization Procedures. Polymerizations were performed in 30 mL glass reactors inside the glovebox for ambient temperature (~25 °C) runs or in 25 mL Schlenk flasks

interfaced to a dual-manifold Schlenk line with an external temperature bath for runs at other temperatures. In a typical procedure for polymerizations of conjugated acryloyl oxazolidinones (AOZ), predetermined amounts of $B(C_6F_5)_3 \cdot THF$ and the appropriate metallocene ester enolate precatalyst in a 1:1 molar ratio were premixed in 5 mL of CH_2Cl_2 and stirred for 10 min to cleanly generate the corresponding cationic ester enolate catalyst.^{19,20,32} The amount of catalyst employed was determined by the [monomer] to [catalyst] ratio specified in the polymerization tables. Monomer (0.737 mmol) was quickly added as a solid to the vigorously stirring solution, and the polymerization was allowed to proceed for 3 h with continuous stirring. For polymerization of vinylloxazolidines (VOZ), monomer (1.06 mmol) was dissolved in the solvent described in the polymerization tables, before addition of initiator as a solid or solution via syringe, and the polymerization was allowed to stir for the time specified in the polymerization tables. After the measured time interval, a 0.2 mL aliquot was taken from the reaction mixture via syringe and quickly quenched into a 4 mL vial containing 0.6 mL of undried “wet” $CDCl_3$ stabilized by 250 ppm of BHT-H; the quenched aliquots were analyzed by 1H NMR to obtain monomer conversion data. The polymerization was immediately quenched after the removal of the aliquot by the addition of 5 mL 5% HCl-acidified methanol. The quenched mixture was precipitated into 50 mL of methanol, stirred for 1 h, filtered or centrifuged, washed with methanol, and dried in a vacuum oven at 50 °C overnight to a constant weight.

For polymerizations carried out at other temperatures, the catalyst (or monomer solution) was loaded in a 25 mL Schlenk flask equipped with a stir bar and a septum cap inside the glovebox. The charged Schlenk flask was taken out of the glovebox, interfaced to a dual-manifold Schlenk line, and immersed in a pre-equilibrated bath at desired temperature. The polymerization was started by adding rapidly the monomer (or catalyst solution) via gastight syringe under positive N_2 pressure. The remaining procedures were the same as those ambient-temperature polymerization runs. Polymerizations using C_5 -ligated metallocenium catalysts for the synthesis of syndiotactic polymers followed the literature procedure.³³

Polymer Characterizations. Gel permeation chromatography (GPC) analyses of the polymers were carried out at 40 °C and a flow rate of 1.0 mL/min, with DMF as the eluent, on a Waters University 1500 GPC instrument equipped with four 5 μ m PL gel columns (Polymer Laboratories) and calibrated using 10 PMMA standards. Chromatograms were processed with Waters Empower software (version 2002); number-average molecular weight (M_n) and molecular weight distribution ($MWD = M_w/M_n$) of polymers were given relative to PMMA standards. Glass transition temperatures (T_g) of the polymers were measured by differential scanning calorimetry (DSC) on a DSC 2920 (TA Instruments). Polymer samples were first heated to 150 °C at 20 °C/min, equilibrated at this temperature for 4 min, then cooled to 30 °C at 20 °C/min, held at this temperature for 4 min, and reheated to 230 °C (for AOZ polymers) or 390 °C (for VOZ polymers) at 10 °C/min. All T_g values were obtained from the second scan, after removing the thermal history from the first heating cycle. Maximum rate decomposition temperatures (T_{max}) and decomposition onset temperatures (T_{onset}) of the polymers were measured by thermal gravimetric analysis (TGA) on a TGA 2950 thermogravimetric analyzer (TA Instruments). Polymer samples were heated from ambient temperatures to 600 °C at a rate of 20 °C/min. Values for T_{max} were obtained from derivative (wt %/°C) vs temperature (°C), while T_{onset} values (initial and end temperatures) were obtained from wt % vs temperature (°C) plots.

Optical rotations were measured on an Autopol III Automatic Polarimeter at 23 °C. The measurements were conducted on 0.2 g/dL polymer solutions in $CHCl_3$. Circular dichroism (CD) spectra were obtained from an Aviv model 202 CD spectrometer. CD analysis was conducted on polymer solutions

with concentrations of 0.2 g/dL in CHCl₃. Powder X-ray diffraction (XRD) analyses were performed on powder samples with a Scintag X2 Advanced Diffraction System using Cu K α ($\lambda = 1.540562 \text{ \AA}$) radiation and a Peltier detector on the diffracted-beam side. In all cases measurements were performed with a step size of 0.02° with 1.2 s per step. The tacticity of (*R*)-PAOZ and (*R*)-PHVOZ was analyzed by ¹³C NMR according to the procedures established for polyacrylamides³⁴ and for the parent PVOZ,¹⁸ respectively. NMR data of the polymers representing each of three classes of the polymers described in this study are listed below.

Poly(*N*-acryloyl-2-oxazolidinone) (PAOZ). ¹H NMR (DMSO-*d*₆, 500 MHz, 100 °C) for PAOZ: δ 4.37 (m, CH₂O, 2H), 3.87 (m, CH₂N, 2H), 3.73, 3.68, 3.60 (m, CH, unresolved triads, 1H), 1.86, 1.71, 1.67, 1.55, 1.48 (m, CH₂, unresolved diads and tetrads, 2H). ¹³C NMR (DMSO-*d*₆, 125 MHz, 100 °C): δ 174.4 (C=O, *rr* + *mr*), 174.3 (C=O, *mm*), 152.7 (C=O, ring), 61.50 (CH₂O), 42.09 (CH₂N), 37.24 (CH), 34.75 (CH₂).

Poly[*N*-acryloyl-(*R*)-4-phenyl-2-oxazolidinone] [(*R*)-PAOZ]. ¹H NMR (DMSO-*d*₆, 500 MHz, 100 °C): δ 7.28 (m, Ar, 5H), 5.38 (m, CH, 1H), 4.64–4.14 (m, CH₂O, 2H), 3.84, 3.76, 3.67 (m, CH, unresolved triads, 1H), 1.88, 1.74, 1.46 (m, CH₂, 2H). ¹³C NMR (DMSO-*d*₆, 125 MHz, 100 °C): δ 174.3 (C=O, *rr* + *mr*), 173.9 (C=O, *mm*), 153.0, (C=O, ring), 139.7, 129.1, 128.3, 125.9 (Ar), 70.18 (CH₂O), 57.98 (CHN), 39.04 (CH), 36.01 (CH₂).

Poly[*N*-vinyl-(*R*)-4-(4-(hexyloxy)phenyl)-2-oxazolidinone] [(*R*)-PHVOZ]. ¹H NMR (500 MHz, CDCl₃, 50 °C): δ 7.62 (bs, Ar, 2H), 6.99 (bs, Ar, 2H), 4.53 (m, 1H), 4.25 (m, 1H), 4.03 (m, 2H), 3.77 (m, 1H), 1.82 (bs, 2H), 1.49 (bs, 2H), 1.35 (bs, 5H), 0.89 (bs, 4H), 0.77 (bs, 1H). ¹³C NMR (CDCl₃, 125 MHz, 50 °C): δ 159.6 (C–O), 158.0 (C=O, *mmmm*), 132.4, 129.6, 115.2 (Ar), 70.26 (CH₂O), 68.24 (CH₂O), 56.23 (CHN), 48.54 (CH), 35.64 (CH₂), 31.60 (CH₂), 29.36 (CH₂), 25.84 (CH₂), 22.56 (CH₂), 13.90 (CH₃).

Results and Discussion

Stereospecific Coordination Polymerization of Chiral Acryloyl Oxazolidinones. As a control and test to examine the compatibility of the oxazolidinone functionality attached to the acryloyl monomer with the cationic metallocenium coordination catalyst, we first polymerized the parent unsubstituted, prochiral acryloyl-2-oxazolidinone (AOZ) with *rac*-**1** at ambient temperature. In accordance with the stereospecific coordination polymerization of *N,N*-diarylacrylamides^{19,20} and *N,N*-dialkylacrylamides^{34a–c} by such metallocene catalysts, the polymerization of AOZ by *rac*-**1** is rapid and produces highly stereoregular, but optically inactive, PAOZ with a near-quantitative isotacticity (*mm*%) of ~99% as determined by ¹³C NMR (see Experimental Section). Since AOZ contains no chiral auxiliary, the observed stereochemistry must be attributed to the catalyst-site-controlled polymerization rendered by the C₂-ligated chiral catalyst.² Next, we polymerized both (*R*)- and (*S*)-AOZ monomers using *rac*-**1** (2 mol %) for 3 h at ambient temperature, achieving quantitative monomer conversions and affording the corresponding isotactic, *optically active* polymers, (*R*)-PAOZ and (*S*)-PAOZ, with MW's = 11.1 and 9.98 kg/mol, respectively (runs 1 and 4, Table 1). The observed MW's are close to the calculated MW of 10.9 kg/mol, and therefore the polymerization shows its control over the resulting polymer MW. The polymers exhibit unimodal MWD's, but they are relatively broad (>2.0), as compared to the typically narrow MWD's (<1.2) observed for poly(alkyl methacrylates) and poly(alkyl acrylamide)s produced by *rac*-**1**.^{30,32,34b} The formation of polymers with relatively broad, unimodal MWD's are normally attributed to the slower rate of chain initiation than the rate of chain propagation for polymerization systems with single-site catalysts.² However, in the case of the

Table 1. Selected Results of Polymerization of (*R* and *S*)-AOZ by Chiral Catalysts **1**^a

run no.	monomer form	catalyst form	conv ^b (%)	10 ³ M _n ^c (g/mol)	MWD ^c (M _w /M _n)	[α] _D ²³ (deg)
1	(<i>R</i>)-AOZ	<i>rac</i> - 1	100	11.1	2.41	−158
2	(<i>R</i>)-AOZ	(<i>R,R</i>)- 1	100	6.77	1.77	−160
3	(<i>R</i>)-AOZ	(<i>S,S</i>)- 1	100	7.88	1.42	−154
4	(<i>S</i>)-AOZ	<i>rac</i> - 1	100	9.98	2.07	+182
5	(<i>S</i>)-AOZ	(<i>R,R</i>)- 1	100	7.23	1.77	+170
6	(<i>S</i>)-AOZ	(<i>S,S</i>)- 1	100	8.27	1.74	+185

^a Carried out in 5 mL of CH₂Cl₂ at ambient temperature (~25 °C); 2 mol % catalyst. ^b Conversion measured by ¹H NMR. ^c Determined by GPC relative to PMMA standards. ^d 0.2 g/dL, CHCl₃.

current system, it could also be attributable to the possibility that the enantiomeric monomer was preferentially polymerized by one enantiomer of the racemic catalyst. To test this hypothesis, we investigated the ability of the (*R,R*)-**1** enantiomer to effect the kinetic resolution polymerization of *rac*-(*R/S*)-AOZ, ideally polymerizing one enantiomer preferentially via a large stereoselectivity factor while resolving the other enantiomerically pure. The actual experiment showed that (*R,R*)-**1** was unable to kinetically resolve (*R/S*)-AOZ, as several aliquots taken during the course of polymerization, when analyzed by chiral HPLC, revealed no enantiomeric excess of the unreacted monomer, demonstrating that each enantiomer of the catalyst polymerizes the enantiomeric monomers with equal efficacy. Furthermore, the specific rotations of the isolated polymers are strikingly similar to their respective monomers. More specifically, [α]_D²³ of (*R*)-AOZ is −159°, while the isolated polymer has the same value (within experimental error) of [α]_D²³ = −158°. Likewise, the specific rotation of (*S*)-AOZ is +159°, and it is +182° for its derived polymer. *Significantly*, the minimal to no change in both magnitude and sign of specific rotations of these polymers, in comparison to their respective monomers, is *drastically different than* the chiral helical polymer examples discussed above, where helix formation resulted in polymers with largely different optical rotations (and sometime in signs as well) than their corresponding monomers.

Efforts in explaining the above results obtained in the polymerization of (*R* and *S*)-AOZ monomers have led to the formulation of the following three hypotheses (possible scenarios): (1) the polymers produced by *rac*-**1** form an equal mixture of right- and left-handed helical structures, where the helicity is determined by the chirality of the catalyst, and therefore the optical activity arising from the secondary structures cancel each other out; (2) one-handed chiral helical polymers are produced, but the helicity is dictated by the chiral side groups of the isotactic polymers; or (3) the polymers produced adopt random-coil conformations, where the stereoregular main chain becomes cryptochiral, and therefore the optical activity is controlled by the chiral auxiliary. Several lines of key evidence detailed below unequivocally disprove hypotheses 1 and 2 and thus show that the third scenario is strongly suggested for the present chiral AOZ polymers.

First, we employed enantiomeric catalysts **1** for the polymerization of (*R* and *S*)-AOZ since the results will reveal if excess one-handed helicity could be formed or not. (*R*)-AOZ was polymerized efficiently by (*R,R*)- and (*S,S*)-**1**, affording the corresponding polymers with MW's = 6.77 and 7.88 kg/mol and MWD's = 1.77 and 1.42, respectively (runs 2 and 3, Table 1). Intriguingly, the specific rotations of all the polymers derived from (*R*)-AOZ are rather similar (i.e., [α]_D²³ varied from a narrow range from −154° to −160°), regardless of the form of the catalyst utilized (runs 1–3). Furthermore, all the polymers

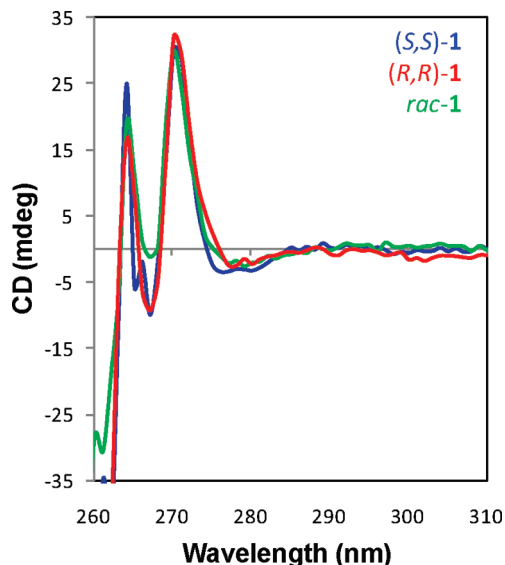


Figure 1. CD spectra of (*R*)-AOZ polymers produced by catalysts (*S,S*)-**1** (blue), (*R,R*)-**1** (red), and *rac*-**1** (green).

show nearly identical Cotton effects, as revealed by their CD spectra (Figure 1), which is in sharp contrast to the chiral helical polymers with one-handed helicity being dictated by the chirality of the catalyst (*vide supra*). Since the polymers derived from (*R*)-AOZ are optically indistinguishable, these results clearly ruled out hypothesis 1, which assumes that each enantiomeric catalyst produces AOZ polymer kinetically trapped in the right- or left-handed, solution-stable helix.

Second, the study of the chiroptical properties of the polymers derived from (*S*)-AOZ using three different forms of catalyst **1** provides additional evidence disproving hypothesis 1. As in the case of the (*R*)-AOZ monomer, (*S*)-AOZ was quantitatively polymerized by the enantiomeric catalysts to isotactic, optically active polymers with MW's = 7.23 and 8.27 kg/mol and MWD's = 1.77 and 1.74 by (*R,R*)- and (*S,S*)-**1**, respectively (runs 5 and 6, Table 1). Identical to the observations with the polymers composed of (*R*)-AOZ, the (*S*)-AOZ-based polymers exhibited rather similar optical rotations, regardless of catalyst form employed (i.e., $[\alpha]^{23}_D = +182^\circ$, $+170^\circ$, and $+185^\circ$ for polymers produced by *rac*-, (*R,R*)-, and (*S,S*)-**1**, respectively) and again nearly identical CD spectra (Figure 2). Hence, these results strongly back the above conclusion (point 1), based on the findings in the polymerization of (*R*)-AOZ, that the enantiomeric catalysts do not convert the enantiomeric AOZ to a kinetically trapped right- or left-handed solution-stable helical polymer.

Third, we ascertained the possibility of the chiral side groups of the polymer dictating helicity (hypothesis 2) due to the observed large change in CD spectra for the isolated polymers, as compared to their respective monomers (Figure 3). Again, this possibility is inconsistent with the observation that there was no chiral amplification and exhibited only minimal differences in specific rotations of the polymers than their respective monomers, as shown by the examples described above. A hypothetical helix–helix stereomutation was also not observed for these polymers, as the specific rotation of the solution did not change immediately after dissolution or after 4 days.

Fourth, the results of our copolymerization studies provide additional evidence for disproof of hypothesis 2. We reasoned that if the chiral auxiliary of the AOZ monomers

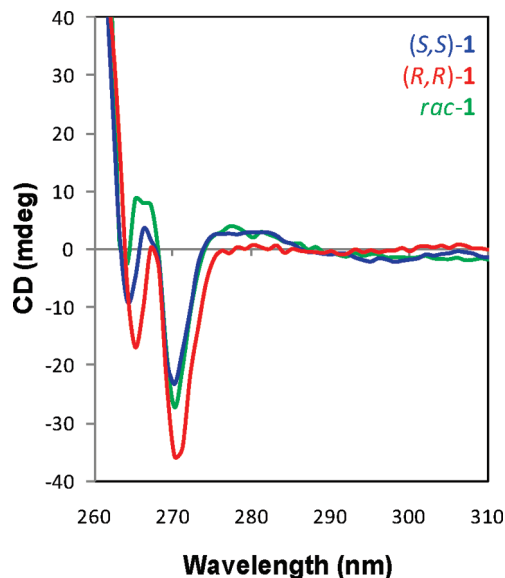


Figure 2. CD spectra of (*S*)-AOZ polymers produced by catalysts (*S,S*)-**1** (blue), (*R,R*)-**1** (red), and *rac*-**1** (green).

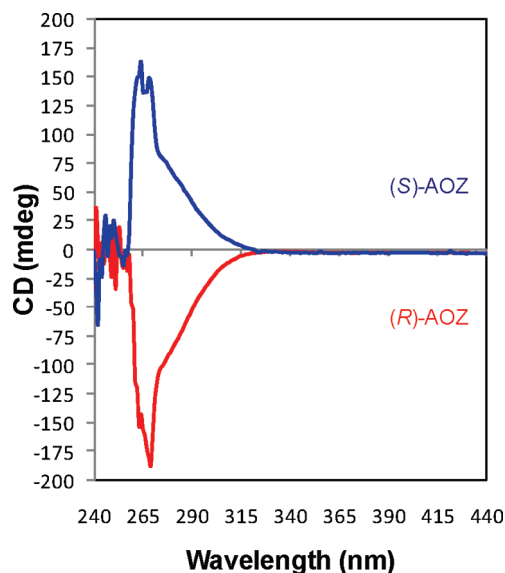


Figure 3. CD spectra of chiral AOZ monomers: (*S*)-AOZ (blue) and (*R*)-AOZ (red).

dictates the formation of a single-handed helical polymer during the course of polymerization, then we can reveal this phenomenon through copolymerizations, specifically, through investigating chiral amplifications manifestable by the majority rules³⁵ or “sergeants and soldiers” effects.³⁶ In both effects, a small chiral bias results in a chiral amplification in the entire polymer chain, leading to highly optically active polymers. To this end, we copolymerized *nonequivalent amounts* of (*R*)- and (*S*)-AOZ by *rac*-**1** (since no kinetic resolution polymerization proceeded, we can employ the *racemic* catalyst directly) (runs 7–9, Table 2). The copolymers with 10, 20, and 40% *ee* of (*R*)-AOZ exhibited very similar MW and MWD, but no chiral amplification was observed in their CD spectra. Furthermore, in examining specific rotations of these polymers, there was just an additive effect in optical rotation, not a chiral amplification. Specifically, the polymers with 10, 20, and 40% *ee* of (*R*)-AOZ had $[\alpha]^{23}_D = -15.9^\circ$, -33.8° , and -70.7° (from run 7 to 9), increasingly

Table 2. Selected Results of Copolymerization of (*R*)- with (*S*)-AOZ by *rac*-1^a

run no.	(<i>R</i>)-AOZ (mol %)	(<i>S</i>)-AOZ (mol %)	conv (%)	10 ³ <i>M</i> _n (g/mol)	MWD (<i>M</i> _w / <i>M</i> _n)	[α] _D ²³ (deg)
7	55	45	100	8.34	1.37	−15.9
8	60	40	100	8.79	1.39	−33.8
9	70	30	100	8.89	1.42	−70.7

^a See footnotes in Table 1 for explanations.**Table 3. Selected Results of Copolymerization of Achiral AOZ with Chiral (*S*)-AOZ by *rac*-1^a**

run no.	(<i>S</i>)-AOZ (%)	AOZ (%)	conv (%)	10 ³ <i>M</i> _n (g/mol)	MWD (<i>M</i> _w / <i>M</i> _n)	[α] _D ²³ (deg)
10	0	100	100	6.03	1.69	0.0
11	4	96	100	7.40	1.41	+18.3
12	10	90	100	7.87	1.43	+28.1
13	20	80	100	8.67	1.43	+35.8

^a See footnotes in Table 1 for explanations.

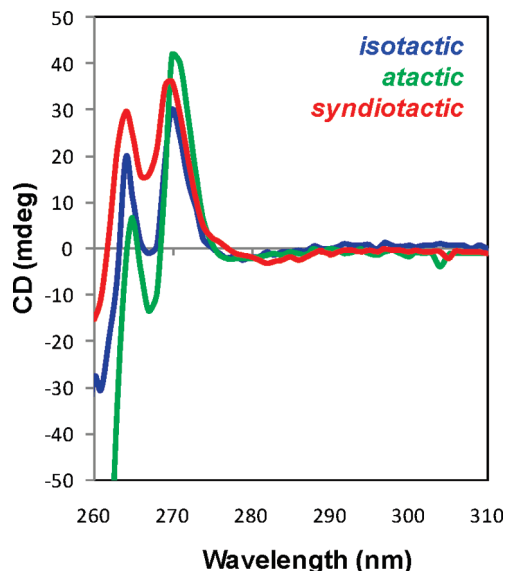
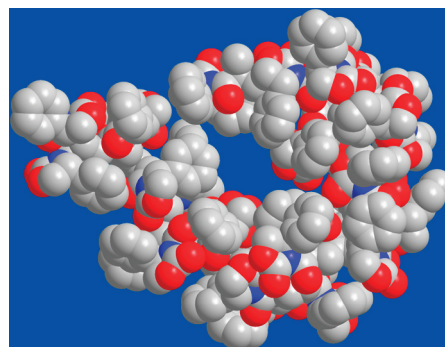
linearly with % *ee*, as was observed in vinyl polymers not forming excess one-handed helicity.³⁷

To examine the ability of these chiral monomers to influence helicity through the “sergeants and soldiers” effect, we copolymerized (*S*)-AOZ with the structurally similar, prochiral acryloyl-2-oxazolidinone (AOZ). As a control, we polymerized AOZ alone with *rac*-1. The optically inactive polymer produced by *rac*-1 exhibited a MW of 6.03 kg/mol and a MWD of 1.69 (run 10, Table 3). Next, we incorporated 4, 10, and 20 mol % of chiral (*S*)-AOZ into the monomer feed, quantitatively producing the corresponding optically active copolymers (runs 11–13, Table 3). However, the specific rotation increased only linearly with incorporation of the chiral monomer, and also no large Cotton effects were observed in the CD spectra, again indicating the lack of chiral amplification. *Overall*, the combination of the results obtained in the homopolymerization of the enantiomeric monomers with the chiral amplification studies, through copolymerization of the mixed chiral–chiral and chiral–achiral monomer feeds, led to the conclusion that the side groups of the repeat units are not bulky enough and too far (three atoms) away from the isotactically placed stereogenic centers of the polymer backbone to sterically induce helicity into the polymer. Instead, random-coil secondary structures form.

Fifth, disproof of hypotheses 1 and 2 by the above four sets of experiments led to the key, third hypothesis that remains consistent with, and thus supported by, all the data: the chiral isotactic AOZ polymers adopt a random-coil conformation, and the optical activity is dictated by the chiral auxiliary. This scenario was further supported by the observation that *all* (*R*)-AOZ polymers with different main-chain stereoconfigurations—specifically, the isotactic polymer by *C*₂-ligated metallocenium catalyst **1**, the syndiotactic polymer by the *C*_s-ligated metallocenium catalysts,³³ and the atactic polymer by the free radical initiator (AIBN)—showed nearly identical Cotton effects in their CD spectra (Figure 4).

Sixth, modeling of isotactic [(*R*)-AOZ]₃₀ by MM2 calculations also led to a random-coil chain secondary structure (Figure 5), thus providing additional support to hypothesis 3. This modeling result is in sharp contrast to the calculated helical structure for isotactic [(*R*)-VOZ]₃₀ (cf. Chart 2), the discussion of which immediately follows.

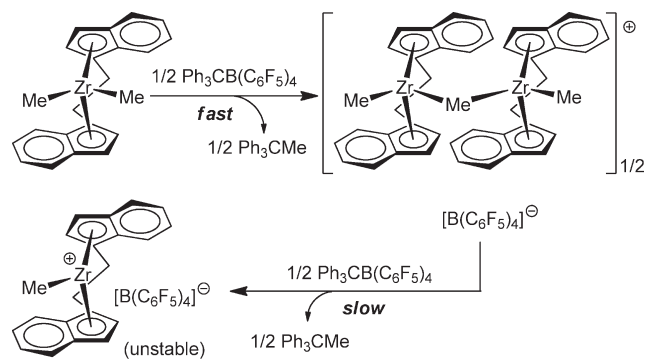
Stereospecific Cationic Polymerization of Chiral Vinyloxazolidinones. As the above studies have shown, the chiral auxiliary of the repeat units in the chiral AOZ polymers are not bulky enough, and too far (three atoms) away from the polymer backbone stereocenters, to sterically induce helicity into the

**Figure 4.** CD spectra of (*R*)-AOZ-derived polymers with different main-chain stereoconfigurations: isotactic polymer (blue), syndiotactic polymer (red), and atactic polymer (green).**Figure 5.** Modeled random-coil structure of [(*R*)-AOZ]₃₀ shown in the space-filling mode. Carbon, nitrogen, and oxygen are shown in gray, blue, and red, respectively; hydrogen atoms are omitted for clarity.

polymer. Accordingly, we reasoned that if we brought the chiral side groups *closer* to the stereocenters of the polymer main chain in polymers derived from nonconjugated *N*-vinyl-4-(*R*)-phenyl-2-oxazolidinone [(*R*)-VOZ], where the chiral auxiliary would now be only two atoms away from the main-chain stereocenters, then the side groups could be effective in rendering solution-stable helical polymers.

However, two *challenges* are present in coordination polymerization of (*R*)-VOZ. First, it is a nonconjugated vinyl monomer, so it cannot be polymerized via a coordination conjugate-addition mechanism by zirconocenium ester enolate catalysts such as **1**.² Second, it is a heteroatom (N,O)-functionalized vinyl monomer, so it cannot be polymerized (at least directly) via a coordination insertion mechanism by metallocenium alkyl catalysts such as *rac*-(EBI)ZrMe⁺MeB-(C₆F₅)₃^{−2}. A potential strategy here is to use protected (coordinated) heteroatom-functionalized vinyl monomers with aluminum Lewis acids, which can be readily removed postpolymerization.³⁸ Initial attempts to polymerize (*R*)-VOZ with *rac*-(EBI)ZrMe₂ activated with 500 equiv of MAO—which we reasoned could not only abstract the methyl group to form the active zirconocenium catalyst species³⁹ but also protect the heteroatoms of (*R*)-VOZ from interfering with the migratory insertion polymerization process—failed to form any isolable polymer after 24 h of reaction. Next, we

Scheme 1. Stepwise Activation of *rac*-(EBI)ZrMe₂ by [Ph₃C][B(C₆F₅)₄]



precomplexed (*R*)-VOZ with 0–3 equiv of ^tBu₃Al and subjected the complexed monomer to polymerization by *rac*-(EBI)ZrMe₂ activated with equimolar B(C₆F₅)₃ [which generates *in situ* the active species, *rac*-(EBI)ZrMe⁺MeB(C₆F₅)₃[−] at ambient temperature or 80 °C for up to 24 h. However, this also yielded no polymer products. We also repeated these polymerization procedures, but using [Ph₃C][B(C₆F₅)₄] as the activator. For the runs using ^tBu₃Al as the complexing agent, no polymerization was observed at various reaction temperature and time. Surprisingly, in the absence of ^tBu₃Al, the polymerization at ambient temperature by *in situ* activation of *rac*-(EBI)ZrMe₂ with equimolar [Ph₃C][B(C₆F₅)₄] proceeded rapidly, with the polymer immediately crashing out of solution.

This intriguing, exciting result raised the question of what is the actual catalyst species responsible for the successful polymerization of (*R*)-VOZ? Note that zirconocenium species such as *rac*-(EBI)ZrMe⁺MeB(C₆F₅)₃[−] are inactive for this polymerization. However, it is known that activation of the metallocene dimethyl precatalyst with [Ph₃C][B(C₆F₅)₄] proceeds in a stepwise fashion: the first step is the rapid methide abstraction to form the transient μ -Me dimer, a result of stabilization of the initially formed metallocene cation by the other half of the neutral dimethyl species, instead of the anion [B(C₆F₅)₄][−], due to its extremely weak coordination nature.⁴⁰ The slower proceeding step is the gradual conversion of the stable dimer to the highly unstable, reactive mononuclear zirconocenium species by the other half of [Ph₃C][B(C₆F₅)₄] (Scheme 1). Thus, the complexity of this activation process presented four possible species being responsible for the observed polymerization activity: the mononuclear zirconocenium cation, the dinuclear cation, the dimethyl precatalyst, and the activator [Ph₃C][B(C₆F₅)₄].

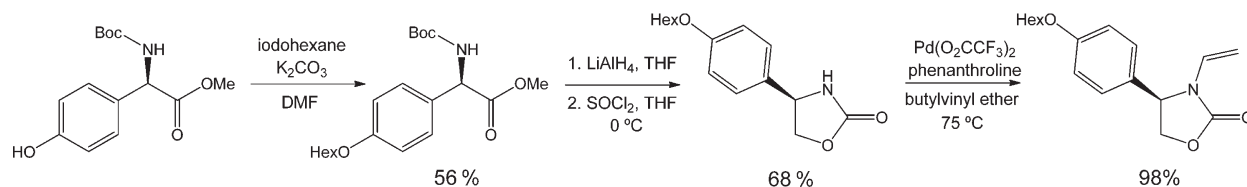
Control experiments subsequently ruled out the neutral precatalyst *rac*-(EBI)ZrMe₂ and the mononuclear zirconocenium cation *rac*-(EBI)ZrMe⁺ as the active species for this polymerization. The independently prepared dinuclear complex⁴⁰ from the reaction of 2 equiv of *rac*-(EBI)ZrMe₂ with 1 equiv of [Ph₃C][B(C₆F₅)₄] also exhibited no polymerization activity. Lastly, we found that addition of a catalytic amount of [Ph₃C][B(C₆F₅)₄] to a toluene solution of (*R*)-VOZ resulted in rapid polymerization with the polymer crashing out of solution, the same phenomenon as seen in the polymerization by *in situ* activation of *rac*-(EBI)ZrMe₂ with equimolar [Ph₃C][B(C₆F₅)₄] (*vide supra*). These results conclusively pointed to [Ph₃C][B(C₆F₅)₄]—intended as the activator for the metallocene precatalyst—as the actual active species responsible for the observed polymerization activity. Unfortunately, all isolated polymers using different {(*R*)-VOZ}:{[Ph₃C][B(C₆F₅)₄]} ratios (5–50), solvents (toluene and CH₂Cl₂), and temperature (0 and 25 °C) are insoluble in

all common organic solvents and concentrated acids tested, even at elevated temperatures (up to the boiling points of the solvents). The polymer yield was held nearly constant of ~60% for runs at {(*R*)-VOZ}:{[Ph₃C][B(C₆F₅)₄]} = 50 at 25 °C for 2 h in toluene or CH₂Cl₂, but the polymerization in THF was almost completely shut down (0.65% yield). The [Ph₃C][B(C₆F₅)₄] initiator can be substituted by other cationic initiators such as BF₃·Et₂O. From a viewpoint of devinylation that plagues the polymerization of the unsubstituted VOZ^{13,15} and other *N*-vinyl heterocyclic monomers¹⁶ using acids, it is intriguing and actually fortunate that instantaneous precipitation of the resulting polymer prevented such devinylation to a large extent, enabling us to achieve the first successful cationic polymerization of VOZ monomers with good polymer yields up to 80% (at 0 °C) and also the first successful synthesis of highly isotactic PVOZ (*vide infra*).

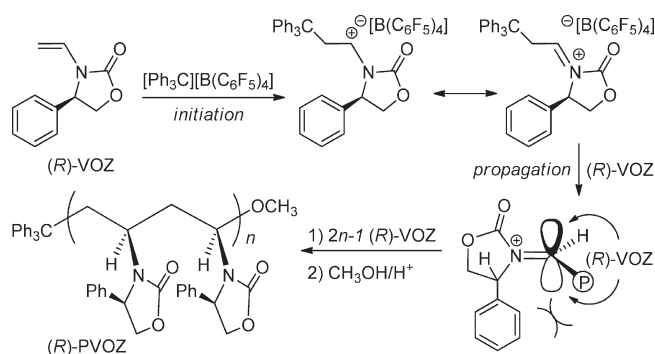
The insolubility of the resulting non-cross-linking (*R*)-PVOZ in all common organic solvents suggests a rigid-rod-like chiral polymer adopting a one-handed helical conformation—as predicted by modeling (cf. Chart 2)—a result of having a highly isotactic backbone stereoconfiguration generated through a novel chiral auxiliary-controlled, isospecific cationic polymerization mechanism. However, to provide concrete evidence for such a polymer structure, the insolubility associated with (*R*)-PVOZ must be solved to allow characterization of the polymer. To this end, we synthesized the *p*-hexyloxy-substituted derivative, (*R*)-4-(4-(hexyloxy)phenyl)-3-vinyl-oxazolidin-2-one [(*R*)-HVOZ], according to Scheme 2, and subsequently investigated its cationic polymerization behavior.

Gratifyingly, (*R*)-HVOZ was also polymerized by [Ph₃C][B(C₆F₅)₄], and the polymerization remained homogeneous during the course of polymerization. The resulting polymers are soluble in common organic solvents, thus enabling characterizations of the polymers by GPC for MW and MWD, NMR for tacticity, and optical rotation and CD for optical activity. However, the isolated polymer yield was very low (6.0%, run 14, Table 4), even after extended reaction time (24 h) at ambient temperature. Nonetheless, the polymer had a relatively narrow MWD of 1.65 and a MW of 7.63 kg/mol. Considering side reactions at ambient temperature often observed for cationic polymerization, we lowered the polymerization temperature to 0 °C (run 15) and −20 °C (run 16), but doing so did not improve the polymer yield. The use of BF₃·Et₂O as initiator enhanced the polymer yield somewhat (to ~10%, run 17) at 25 °C, but variations in polymerization temperature (runs 18 and 19) lowered the yield. Brønsted acids were also examined, including [H(Et₂O)₂]⁺[B(C₆F₅)₄][−] (run 20) and [HN(Me₂)Ph]⁺[B(C₆F₅)₄][−], but the polymer yield was never higher than 10%.

Hypothesizing that devinylation may be the cause for the low polymer yield seen in the cationic polymerization of (*R*)-HVOZ, we investigated the stoichiometric reaction of (*R*)-HVOZ with [Ph₃C][B(C₆F₅)₄]. Indeed, the isolated product from the reaction was (*R*)-4-(4-(hexyloxy)phenyl)oxazolidin-2-one, the devinylation product. Likewise, the polymerization reaction of (*R*)-HVOZ with a catalytic amount of [Ph₃C][B(C₆F₅)₄] led to (after quenching the reaction, separating the MeOH insoluble polymer fraction, and removing the solvent) isolation of almost exclusively the oxazolidinone. Although acid-catalyzed decomposition of *N*-vinyl heterocyclic monomers via devinylation,^{13,15} even in the solid state,¹⁶ is known, it was surprising to see the sharp contrast in the extent of the monomer decomposition between the heterogeneous polymerization of (*R*)-VOZ and the homogeneous polymerization of (*R*)-HVOZ. A further study through monitoring the reaction of [Ph₃C][B(C₆F₅)₄] with 5 equiv

Scheme 2. Outlined Synthesis of (*R*)-HVOZTable 4. Selected Results of Cationic Polymerization of (*R*)-HVOZ^a

run no.	initiator	temp (°C)	yield (%)	10 ³ M _n (g/mol)	MWD (M _w /M _n)
14	[Ph ₃ C][B(C ₆ F ₅) ₄]	25	6.0	7.63	1.65
15	[Ph ₃ C][B(C ₆ F ₅) ₄]	0	2.0	7.11	1.69
16	[Ph ₃ C][B(C ₆ F ₅) ₄]	-20	5.8	5.20	1.81
17	BF ₃ ·Et ₂ O	25	9.5	6.53	1.60
18	BF ₃ ·Et ₂ O	0	6.9	6.68	1.79
19	BF ₃ ·Et ₂ O	-20	6.3	5.26	1.78
20	[H(Et ₂ O) ₂][B(C ₆ F ₅) ₄]	25	9.5	7.31	1.64

^aSee footnotes in Table 1 for explanations.Scheme 3. Proposed Chiral Auxiliary-Controlled Isospecific Cationic Polymerization of (*R*)-(H)VOZ

of (*R*)-HVOZ revealed a valuable insight: isotactic polymer was formed initially, but over time the backbone methylene proton signals corresponding to an isotactic configuration disappeared, and the proton signal for the oxazolidinone appeared. Hence, this experiment showed that some polymerization initially occurs, followed by decomposition to give oxazolidinone, thus competing with the direct devinylation of the monomer. This valuable insight also explains the drastic difference in polymer yields between the polymerizations of (*R*)-VOZ and (*R*)-HVOZ: the hexyloxy substitution in (*R*)-HVOZ should have minimal to none effects on the rate of monomer devinylation, but instead it is the insolubility of (*R*)-PVOZ, upon forming and crashing out of solution, that prevents it from decomposition. Obviously, this mechanism of devinylation prevention does not apply to the soluble (*R*)-PHVOZ.

On the other hand, the solubility of (*R*)-PHVOZ allowed us to investigate its tacticity and optical properties, despite the observed low polymer yield. As anticipated, analysis of the ¹³C NMR spectrum of (*R*)-PHVOZ produced by [Ph₃C][B(C₆F₅)₄] at ambient temperature clearly reveals its high isotacticity, as evidenced by the single *mmmm* pentad peak in the C=O region which is collaborated by the single methine and methylene backbone carbon peaks (Figure 6). Outlined in Scheme 3 is the proposed chiral auxiliary-controlled isospecific cationic polymerization for the production of isotactic, chiral vinyl oxazolidinone-functionalized vinyl polymers, where the concept of stereocontrol in repeated vinyl additions is analogous to the stereocontrol observed in the free radical polymerization of chiral acrylamides.^{10–12} More importantly, combination of this near-quantitatively

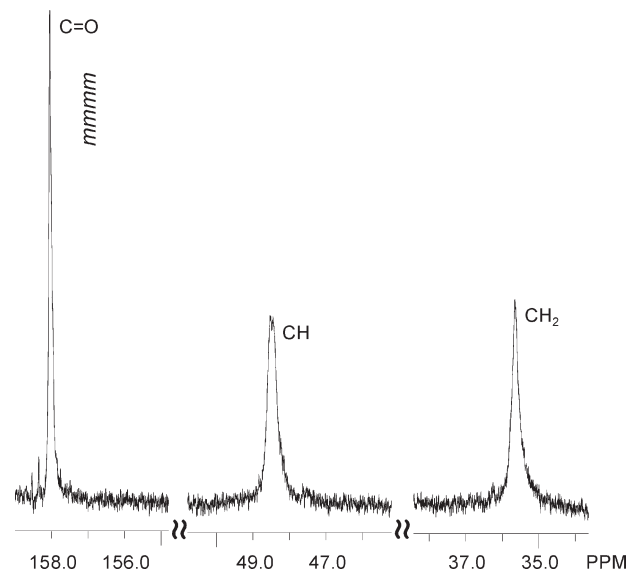


Figure 6. Carbonyl as well as main-chain CH and CH₂ regions in the ¹³C NMR (125 MHz, CDCl₃, 50 °C) of (*R*)-PHVOZ produced by [Ph₃C][B(C₆F₅)₄] at ambient temperature.

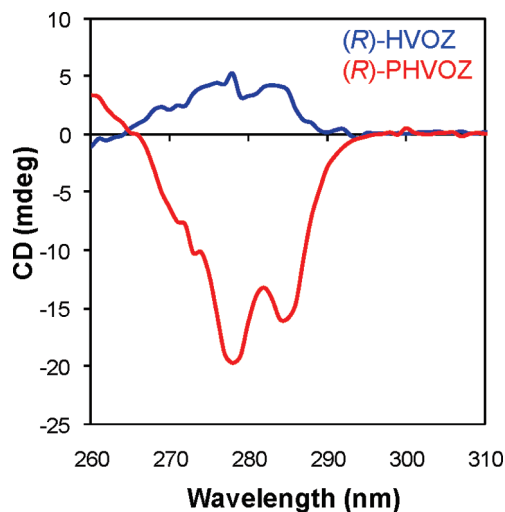


Figure 7. CD spectra of monomer (*R*)-HVOZ (blue) and polymer (*R*)-PHVOZ (red).

isotactic placement of the stereogenic centers of the polymer main chain with the chiral side groups located near those stereocenters of the backbone rendered one-handed helicity for (*R*)-PVOZ and (*R*)-PHVOZ. Owing to the insolubility of (*R*)-PVOZ, its helical structure was only inferred by modeling (cf. Chart 2). Thanks to the solubility of (*R*)-PHVOZ, the helical structure is now directly supported by the experimental results, including the greatly changed specific rotation, in both magnitude and sign, in going from the monomer (*R*)-HVOZ to the polymer (*R*)-PHVOZ (−44.8 °C to +156; run 14, Table 4) as well as the drastically different CD spectra between the monomer and the polymer (Figure 7). Each of

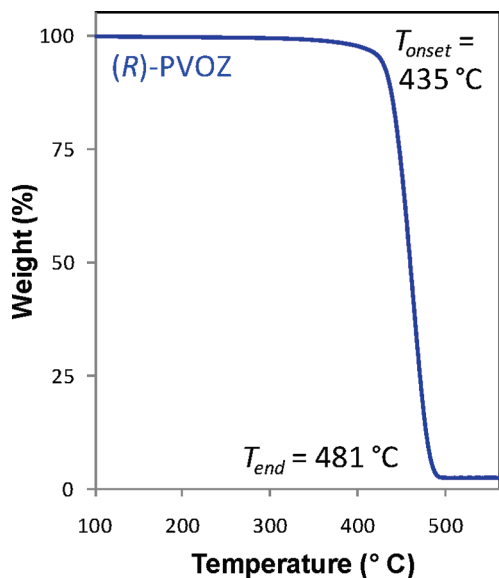


Figure 8. TGA plot of (*R*)-PVOZ produced by $[\text{Ph}_3\text{C}][\text{B}(\text{C}_6\text{F}_5)_4]$ in CH_2Cl_2 .

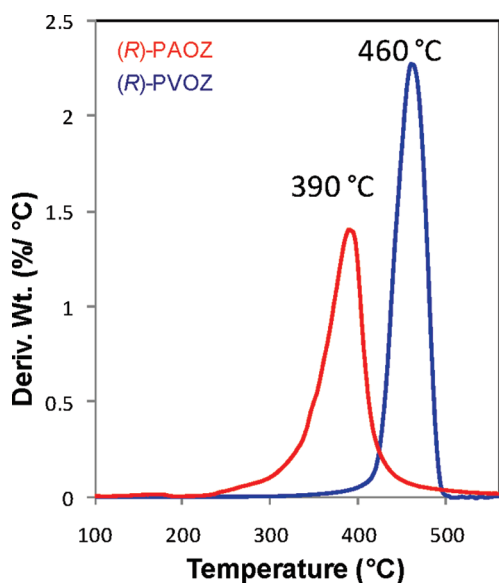


Figure 9. TGA derivative plots of (*R*)-PAOZ (red, run 3, Table 1) and (*R*)-PVOZ produced by $[\text{Ph}_3\text{C}][\text{B}(\text{C}_6\text{F}_5)_4]$ in CH_2Cl_2 .

these observables represents chiral amplifications characteristic of helical structure formation.

Physical Properties of Stereoregular (*R*)-PAOZ and (*R*)-PVOZ. Polymer thermal transition, decomposition, and crystallinity were analyzed by DSC, TGA, and XRD, respectively, and comparisons were made between the rigid-rod-like helical polymer (*R*)-PVOZ, produced via isospecific cationic polymerization by $[\text{Ph}_3\text{C}][\text{B}(\text{C}_6\text{F}_5)_4]$, and the random-coil polymer (*R*)-PAOZ, produced via isospecific coordination polymerization by catalyst **1**. In the DSC trace, no T_g was observed for (*R*)-PVOZ in the conditions employed, which is not surprising for such a highly isotactic and crystalline polymer.^{34b,c} On the other hand, (*R*)-PAOZ exhibited a high T_g of 196 °C. In the TGA trace, (*R*)-PVOZ showed a very narrow, one-step decomposition window with high decomposition temperatures of $T_{\text{initial}} = 435$ °C, $T_{\text{end}} = 481$ °C (Figure 8), and $T_{\text{max}} = 460$ °C. In comparison, (*R*)-PAOZ showed in its TGA trace a relatively broader, one-step decomposition window, with much lower decomposition

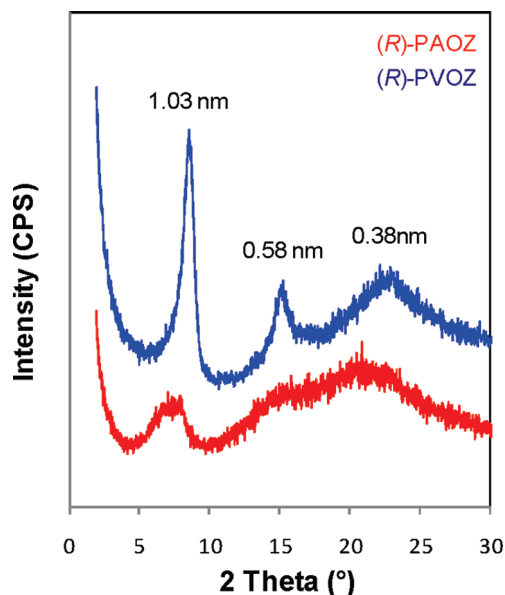


Figure 10. Overlay XRD plots of (*R*)-PAOZ (red, run 3, Table 1) and (*R*)-PVOZ produced by $[\text{Ph}_3\text{C}][\text{B}(\text{C}_6\text{F}_5)_4]$ in CH_2Cl_2 .

temperatures of $T_{\text{initial}} = 351$ °C, $T_{\text{end}} = 412$ °C, and $T_{\text{max}} = 390$ °C (Figure 9).

The XRD plots show significant differences in the crystallinity in the as-quenched polymers, (*R*)-PVOZ and (*R*)-PAOZ (Figure 10). Although both isotactic polymers exhibit three distinct scattering peaks [d spacing: 1.03, 0.58, and 0.38 nm for (*R*)-PVOZ], the sharpness and intensity of the scattering peaks of (*R*)-PVOZ is significantly greater, indicating a higher degree of crystallinity, as compared to (*R*)-PAOZ. Overall, these characterizations demonstrated that the chiral isotactic vinyl polymer (*R*)-PVOZ is considerably more thermally stable and more crystalline than the chiral isotactic acrylamide polymer (*R*)-PAOZ, characteristics attributable to the rigid-rod-like, helical structure of the chiral vinyl polymer.

Conclusions

Chiral oxazolidinone-functionalized alkenes have been successfully polymerized at ambient temperature in a stereospecific fashion, leading to the corresponding highly isotactic, optically active polymers. Depending on whether the monomer is conjugated or not, the polymerization proceeds through one of two mechanisms. For conjugated chiral acryloyl oxazolidinones, (*R* or *S*)-AOZ, *isospecific coordination* polymerization is brought about by chiral catalysts **1** in both racemic and enantiomeric forms. This polymerization is catalyst-site controlled, producing highly isotactic, optically active polymers (*R* or *S*)-PAOZ. Owing to the nature of chiral catalyst site control, the coordination polymerization of the parent AOZ without the chiral side group also affords PAOZ with nearly quantitative isotacticity. These oxazolidinone-functionalized, chiral isotactic poly(acrylamide)s adopt a random-coil structure, thus having a cryptochiral chain and exhibiting no chiral amplifications; their optical activity arises solely from the chiral auxiliary. These results are rationalized by the chiral side groups in these chiral poly(acrylamide)s not being sufficiently bulky and located too far away from the isotactically placed stereocenters of the main chain to induce sterically a solution-stable helical conformation.

In order to polymerize nonconjugated chiral vinyl oxazolidinones, we successfully developed a novel ambient-temperature *isospecific cationic* polymerization using Lewis and Brønsted acids.

This polymerization is chiral auxiliary controlled and also produces highly isotactic, optically active polymers, (*R*)-PVOZ and (*R*)-PHVOZ. However, in sharp contrast to the chiral acrylamide polymers, these vinyl polymers adopt a solution-stable helical conformation, thereby manifesting substantial chiral amplifications. Both modeling of the insoluble (*R*)-PVOZ and experimental results obtained from the soluble (*R*)-PHVOZ polymer have yielded the same result: a chiral helical structure. Synthetically, the facile acid-catalyzed devinylation presented a major challenge to the homogeneous, stereospecific cationic polymerization of (*R*)-HVOZ, thus severally limiting its polymer yield. Efforts are underway to search for more effective strategies to eliminate or largely suppress such side reactions.

The chiral helical vinyl polymers synthesized herein are of particular interest for two key reasons. First, they effectively assemble two elements of polymer local chirality—side-chain chirality and main-chain chirality—into global chirality in the form of excess one-handed helicity. Second, these N,O-functionalized chiral vinyl polymers represent chiral variants of structurally similar PVP, the currently most widely employed effective ligand/stabilizer in transition-metal nanocluster chemistry. Such globally assembled helical chiral polymers already showed their superior physical properties such as having considerably higher thermal decomposition temperatures and polymer crystallinity as compared to the random coil chiral acryloyl polymers having similarly high main-chain stereoregularity. Our research in utilizing both classes of chiral polymers synthesized herein as chiral ligands/stabilizers for transition-metal nanoclusters and their subsequent asymmetric catalysis is currently underway, the results of which will appear elsewhere in due course.

Acknowledgment. This work was supported by the National Science Foundation (NSF-0756633). We thank Prof. Alan Kennan of CSU for access to his CD spectrometer and Boulder Scientific Co. for the research gifts of $B(C_6F_5)_3$, $[Ph_3C]^+[B(C_6F_5)_4]^-$, and $[HN(Me_2)Ph]^+[B(C_6F_5)_4]^-$.

References and Notes

- (1) (a) Yashima, E. *Polym. J.* **2010**, *42*, 3–16. (b) Ikai, T.; Okamoto, Y. *Chem. Rev.* **2009**, *109*, 6077–6101. (c) Yashima, E.; Maeda, K.; Iida, H.; Furusho, Y.; Nagai, K. *Chem. Rev.* **2009**, *109*, 6102–6211. (d) Okamoto, Y. *J. Polym. Sci., Part A: Polym. Chem.* **2009**, *47*, 1731–1739. (e) Yashima, E.; Maeda, K.; Furusho, Y. *Acc. Chem. Res.* **2008**, *41*, 1166–1180. (f) Yashima, E.; Maeda, K. *Macromolecules* **2008**, *41*, 3–12. (g) Okamoto, Y.; Ikai, T. *Chem. Soc. Rev.* **2008**, *37*, 2593–2608. (h) Hembury, G. A.; Borovkov, V. V.; Inoue, Y. *Chem. Rev.* **2008**, *108*, 1–73. (i) Yamamoto, C.; Okamoto, Y. *Bull. Chem. Soc. Jpn.* **2004**, *77*, 227–257. (j) Nakano, T.; Okamoto, Y. *Chem. Rev.* **2001**, *101*, 4013–4038. (k) Cornelissen, J. J. L. M.; Rowan, A. E.; Nolte, R. J. M.; Sommerdijk, N. A. J. M. *Chem. Rev.* **2001**, *101*, 4029–4070. (l) Okamoto, Y.; Nakano, T. *Chem. Rev.* **1994**, *94*, 349–372. (m) Wulff, G. *Polym. News* **1991**, *16*, 167–173. (n) Okamoto, Y.; Yashima, E. *Prog. Polym. Sci.* **1990**, *15*, 263–298. (o) Wulff, G. *Angew. Chem., Int. Ed. Engl.* **1989**, *28*, 21–37. (p) Farina, M. *Top. Stereochem.* **1987**, *17*, 1–111. (q) Pino, P. *Adv. Polym. Sci.* **1965**, *4*, 393–456.
- (2) Recent reviews: (a) Chen, E. Y.-X. *Chem. Rev.* **2009**, *109*, 5157–5214. (b) Chen, E. Y.-X. *Dalton Trans.* **2009**, 8784–8793.
- (3) Selected reviews: (a) Finney, E. E.; Finke, R. G. *J. Colloid Interface Sci.* **2008**, *317*, 351–374. (b) Starkey-Ott, L.; Finke, R. G. *Coord. Chem. Rev.* **2007**, *251*, 1075–1100. (c) Astruc, D.; Lu, F.; Aranzues, J. R. *Angew. Chem., Int. Ed.* **2005**, *44*, 7852–7872. (d) Aiken, J. D., III; Finke, R. G. *J. Mol. Catal. A: Chem.* **1999**, *145*, 1–44.
- (4) Selected recent examples: (a) Yamamoto, T.; Suginome, M. *Angew. Chem., Int. Ed.* **2009**, *48*, 539–542. (b) Reggelin, M.; Doerr, S.; Klusmann, M.; Schultz, M.; Holbach, M. *Proc. Natl. Acad. Sci. U.S.A.* **2004**, *101*, 5461–5466. (c) Reggelin, M.; Schultz, M.; Holbach, M. *Angew. Chem., Int. Ed.* **2002**, *41*, 1614–1617.
- (5) Selected recent examples: (a) Starkey-Ott, L.; Hornstein, B. J.; Finke, R. G. *Langmuir* **2006**, *22*, 9357–9367. (b) Seo, D.; Park, J. C.; Song, H. *J. Am. Chem. Soc.* **2006**, *128*, 14863–14870. (c) Wiley, B.; Sun, Y.; Mayers, B.; Xia, Y. *Chem.—Eur. J.* **2005**, *11*, 454–463.
- (6) Gao, D.; Schefzick, S.; Lipowitz, K. B. *J. Am. Chem. Soc.* **1999**, *121*, 9481–9482.
- (7) Pino, P.; Lorenzi, G. P. *J. Am. Chem. Soc.* **1960**, *82*, 4745–4747.
- (8) Ager, D. J.; Prakash, I.; Schaad, D. R. *Aldrichim. Acta* **1997**, *30*, 3–12.
- (9) Recent reviews: (a) Satoh, K.; Kamigaito, M. *Chem. Rev.* **2009**, *109*, 5120–5156. (b) Kamigaito, M.; Satoh, K. *Macromolecules* **2008**, *41*, 269–276.
- (10) Mero, C. L.; Porter, N. A. *J. Org. Chem.* **2000**, *65*, 775–781.
- (11) Porter, N. A.; Breyer, R.; Swann, E.; Nally, J.; Pradhan, J.; Allen, T.; McPhil, A. T. *J. Am. Chem. Soc.* **1991**, *113*, 7002–7010.
- (12) Porter, N. A.; Allen, T. R.; Breyer, R. A. *J. Am. Chem. Soc.* **1992**, *114*, 7676–7683.
- (13) Endo, T.; Numazawa, R.; Okawara, M. *Makromol. Chem.* **1971**, *146*, 247–256.
- (14) Drechsel, E. K. *J. Org. Chem.* **1957**, *22*, 849–851.
- (15) Kutner, A. *J. Org. Chem.* **1961**, *26*, 3495–3498.
- (16) For examples: (a) Meyers, R. A.; Christman, E. M. *J. Polym. Sci., Part A-1* **1968**, *6*, 945–950. (b) Lashua, S. C.; Hibbard, B. B. US Pat. 3,284,414, 1966.
- (17) (a) Walles, W. E.; Tousignant, W. F.; Houtman, T., Jr. US Pat. 3,539,540, 1970. (b) Bakke, W. W. US Pat. 3,033,829, 1962.
- (18) Trumbo, D. L. *Polym. Bull.* **1993**, *31*, 569–575.
- (19) Miyake, G. M.; Mariott, W. R.; Chen, E. Y.-X. *J. Am. Chem. Soc.* **2007**, *129*, 6724–6725.
- (20) Miyake, G. M.; Chen, E. Y.-X. *Macromolecules* **2008**, *41*, 3405–3416.
- (21) Wulff, G.; Zweeking, U. *Chem.—Eur. J.* **1999**, *5*, 1898–1904.
- (22) Chelation of a cationic zirconocene center to both carbonyls of *N*-acryloyl-2-oxazolidinone has been demonstrated in: (a) Bondar, G. V.; Aldea, R.; Levy, C. J.; Jaquith, J. B.; Collins, S. *Organometallics* **2000**, *19*, 947–949. (b) Jaquith, J. B.; Levy, C. J.; Bondar, G. V.; Wang, S.; Collins, S. *Organometallics* **1998**, *17*, 914–925. (c) Lin, S.; Bondar, G. V.; Levy, C. J.; Collins, S. *J. Org. Chem.* **1998**, *63*, 1885–1892.
- (23) (a) Gao, Y.; Wei, C.-Q.; Burke, T. R. *Org. Lett.* **2001**, *3*, 1617–1620. (b) Nicolas, E.; Russell, K. C.; Knollenberg, J.; Hruby, V. J. *J. Org. Chem.* **1993**, *58*, 7565–7571.
- (24) Evans, D. A.; Miller, S. J.; Lectka, T.; von Matt, P. *J. Am. Chem. Soc.* **1999**, *121*, 7559–7573.
- (25) Gaulon, C.; Dhal, R.; Dujardin, G. *Synthesis* **2003**, *14*, 2269–2272.
- (26) Jutz, P.; Müller, C.; Stammer, A.; Stammer, H. *Organometallics* **2000**, *19*, 1442–1444.
- (27) (a) Ning, Y.; Caporaso, L.; Correa, A.; Gustafson, L. O.; Cavallo, L.; Chen, E. Y.-X. *Macromolecules* **2008**, *41*, 6910–6919. (b) Kim, Y.-J.; Bernstein, M. P.; Galiano Roth, A. S.; Romesber, F. E.; Williard, P. G.; Fuller, D. J.; Harrison, A. T.; Collum, D. B. *J. Org. Chem.* **1991**, *56*, 4435–4439.
- (28) (a) Grossman, R. B.; Doyle, R. A.; Buchwald, S. L. *Organometallics* **1991**, *10*, 1501–1505. (b) Collins, S.; Kuntz, B. A.; Taylor, N. J.; Ward, D. G. *J. Organomet. Chem.* **1988**, *342*, 21–29.
- (29) Diamond, G. M.; Jordan, R. F.; Petersen, J. L. *J. Am. Chem. Soc.* **1996**, *118*, 8024–8033.
- (30) Bolig, A. D.; Chen, E. Y.-X. *J. Am. Chem. Soc.* **2004**, *126*, 4897–4906.
- (31) LoCoco, M. D.; Jordan, R. F. *J. Am. Chem. Soc.* **2004**, *126*, 13918–13919.
- (32) Rodriguez-Delgado, A.; Chen, E. Y.-X. *Macromolecules* **2005**, *38*, 2587–2594.
- (33) Zhang, Y.; Ning, Y.; Caporaso, L.; Cavallo, L.; Chen, E. Y.-X. *J. Am. Chem. Soc.* **2010**, *132*, 2695–2709.
- (34) (a) Miyake, G. M.; Caporaso, L.; Cavallo, L.; Chen, E. Y.-X. *Macromolecules* **2009**, *42*, 1462–1471. (b) Mariott, W. R.; Chen, E. Y.-X. *Macromolecules* **2005**, *38*, 6822–6832. (c) Mariott, W. R.; Chen, E. Y.-X. *Macromolecules* **2004**, *37*, 4741–4743. (d) Kobayashi, M.; Okuyama, S.; Ishizone, T.; Nakahama, S. *Macromolecules* **1999**, *32*, 6466–6477. (e) Xie, X.; Hogen-Esch, T. E. *Macromolecules* **1996**, *29*, 1746–1752. (f) Bulai, A.; Jimeno, M. L.; de Queiroz, A.-A. A.; Gallardo, A.; Roman, J. S. *Macromolecules* **1996**, *29*, 3240–3246.
- (35) Jha, S. K.; Cheon, K.; Green, M. M.; Selinger, J. V. *J. Am. Chem. Soc.* **1999**, *121*, 1665–1673.
- (36) Green, M. M.; Reidy, M. P.; Johnson, R. J.; Darling, G.; Oleary, D. J.; Willson, G. *J. Am. Chem. Soc.* **1989**, *111*, 6452–6454.
- (37) (a) Green, M. M.; Jha, S. K. *Chirality* **1997**, *9*, 424–427. (b) Pino, P.; Ciardelli, F.; Motagnoli, G.; Pieroni, O. *J. Polym. Sci., Part B: Polym. Lett.* **1967**, *5*, 307–311.
- (38) Boffa, L. S.; Novak, B. M. *Chem. Rev.* **2000**, *100*, 1479–1493.
- (39) Chen, E. Y.-X.; Marks, T. J. *Chem. Rev.* **2000**, *100*, 1391–1434.
- (40) (a) Chen, E. Y.-X.; Metz, M. V.; Li, L.; Stern, C. L.; Marks, T. J. *J. Am. Chem. Soc.* **1997**, *120*, 6287–6305. (b) Bochmann, M.; Lancaster, S. J. *Angew. Chem., Int. Ed. Engl.* **1994**, *33*, 1634–1637.